Paper 185

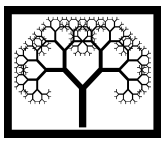

©Civil-Comp Press, 2005.
Proceedings of the Tenth International Conference
on Civil, Structural and Environmental
Engineering Computing,
B.H.V. Topping (Editor),
Civil-Comp Press, Stirling, Scotland.

# A Micro-Mechanical Model for the Homogenized Limit Analysis of Out-Of-Plane Loaded Masonry Walls

**G. Milani†, P.B. Lourenço‡ and A. Tralli†**
**† Department of Engineering**
**University of Ferrara, Ferrara, Italy**
**‡ Department of Civil Engineering**
**University of Minho, Guimarães, Portugal**

## Abstract

The paper presents a novel micro-mechanical model for the homogenized limit analysis of out-of-plane loaded masonry walls. In the framework of homogenization combined with limit analysis, masonry thickness is subdivided in several layers and for each layer polynomial distributions for the stress fields are a-priori assumed inside a fixed number of sub-domains. In this way, a simple linear optimisation problem is derived in order to obtain out-of-plane homogenized failure surfaces of masonry. Then, the surfaces so recovered are implemented in FE limit analysis codes for upper and lower bound analyses on entire masonry panels out-of-plane loaded. Some of these numerical investigations are reported in the paper in order to show the reliability of the results obtained (in terms both of collapse loads and failure mechanisms) in comparison with experimental evidences.

**Keywords:** masonry, homogenization, limit analysis, out-of-plane loads, lower bound, upper bound.

## 1 Introduction

The prediction of the ultimate load bearing capacity of masonry walls out-of-plane loaded is technically very interesting. In fact, out-of-plane failures are mostly related to seismic and wind loads and earthquake surveys have demonstrated that the lack of out-of-plane strength is a primary cause of failure in the most traditional forms of masonry. This fact is confirmed in the case of historical buildings, where the façades are often characterized by a relative small thickness (see for instance [1]). Furthermore, many damages suffered by old masonry buildings during earthquakes might be ascribed to out-of-plane collapses. Another important aspect to underline is that masonry structures are usually subjected simultaneously to in-plane compressive vertical loads and out-of-plane actions. As shown by experimentations,

these loads increase not only the ultimate out-of-plane strength but also the ductility of masonry.

Furthermore, many laboratory tests conducted on brick masonry walls subjected to lateral loads, have demonstrated that failure takes place along a definite pattern of lines, so inspiring approximate analytical solutions based on the yield line theory [2]. Up to now, the yield line method seems the only suitable to be applied in practice for the evaluation of the ultimate load bearing capacity of masonry out-of-plane loaded. Furthermore, probably for its theoretical simplicity, it has been adopted by many codes, as for instance BS 5628 [3] and EC 6 [4].

All codes of practice employ only out-of-plane masonry strengths along the two principal material directions (which are experimentally available directly), leading unavoidably to an approximate estimation of the collapse load, which does not take into account brickwork torsion strength contribute.

For this reason, limit analysis combined with homogenization technique seems a powerful tool able to predict masonry behaviour at collapse. Furthermore, this approach both requires only a reduced number of material parameters and allows to avoid independent modelling of units and mortar. In addition, it provides limit multipliers of loads, failure mechanisms and the stress distribution at collapse. On the other hand, an evident drawback of homogenization is that it requires to solve (usually by means of FE techniques) a field problem on the elementary cell and different loading conditions require different expensive simulations.

The simple model presented in this paper allows to avoid a FE cell discretization; the elementary cell is subdivided along the thickness in several layers, for each layer fully equilibrated stress fields are assumed, a-priori fixing polynomial expressions for the stress tensor components in a finite number of sub-domains, imposing the continuity of the stress vector on the interfaces and anti-periodicity conditions on the boundary surface. In the framework of limit analysis, such stress distribution represents a statically admissible micro stress field and leads to a linear optimization problem. Out-of-plane failure surfaces of masonry are easily recovered and then implemented in FE limit analysis codes (both upper and lower bound) for the homogenized limit analysis of entire panels out-of-plane loaded.

In Section 2, after a brief review of the homogenization theory combined with limit analysis, the fully equilibrated micro-mechanical model is discussed in detail.

In Section 3 the FE triangular elements employed for the upper and lower bound limit analyses are briefly recalled. The lower bound approach is based on the equilibrated triangular element by Hellan [5] and Herrmann [6], whereas the upper bound is based on the triangular element by Munro and Da Fonseca [7].

In Section 4, two different panels out-of-plane loaded [8] [9] are analyzed with the model at hand in order to show the capabilities of the approach if compared with experimental evidences.

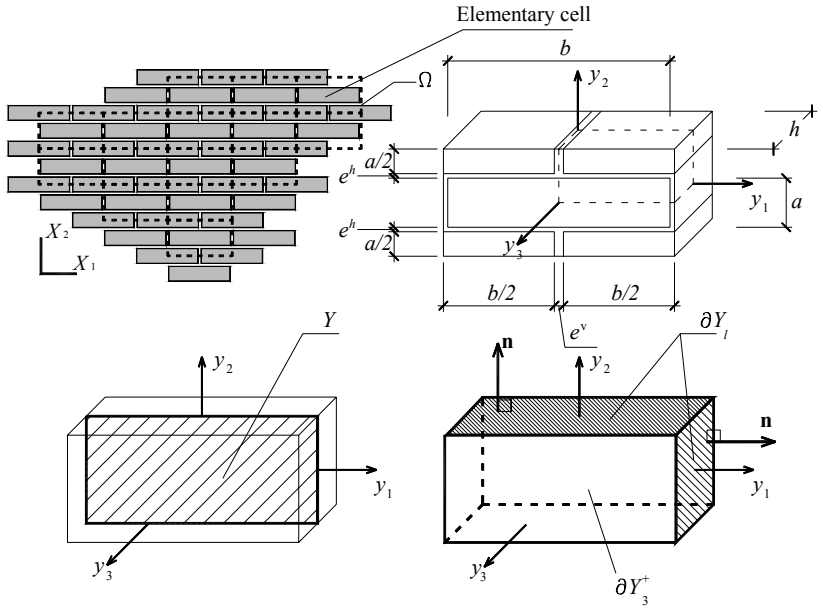


Figure 1: Periodic structure ($X_1 - X_2$: macroscopic frame of reference) and elementary cell ($y_1 - y_2 - y_3$: local frame of reference)

## 2 The micro-mechanical model proposed

A masonry wall $\Omega$ constituted by a periodic arrangement of bricks and mortar disposed in stretcher bond texture is considered. As it as been shown by Suquet in [10], homogenization techniques combined with limit analysis can be applied for the evaluation of the homogenized out-of-plane strength domain $S^{\text{hom}}$ of masonry.

Under the assumption of perfect plasticity and associated flow rule for the constituent materials and in the framework of the lower bound limit analysis theorem, $S^{\text{hom}}$ can be derived by means of the following (non-linear) optimization problem (see also Figure 1):

$$S^{\text{hom}} = \left\{ (\mathbf{M},\mathbf{N}) \,|\, \left\{ \begin{array}{ll} \mathbf{N} = \dfrac{1}{|Y|}\displaystyle\int_{Y\times h} \boldsymbol{\sigma} dV & (a) \\ \mathbf{M} = \dfrac{1}{|Y|}\displaystyle\int_{Y\times h} y_3 \boldsymbol{\sigma} dV & (b) \\ div\boldsymbol{\sigma} = \mathbf{0} & (c) \\ [\![\boldsymbol{\sigma}]\!]\mathbf{n}^{\text{int}} = \mathbf{0} & (d) \\ \boldsymbol{\sigma}\mathbf{n} \quad \text{anti-periodic} \quad \text{on} \quad \partial Y_l & (e) \\ \boldsymbol{\sigma}(\mathbf{y}) \in S^m \quad \forall \mathbf{y} \in Y^m \;;\; \boldsymbol{\sigma}(\mathbf{y}) \in S^b \quad \forall \mathbf{y} \in Y^b & (f) \end{array} \right\} \right\} \tag{1}$$

where:

- $\mathbf{N}$ and $\mathbf{M}$ are the macroscopic in-plane (membrane forces) and out-of-plane (bending moments) tensors;
- $\boldsymbol{\sigma}$ denotes the microscopic stress tensor and $\mathbf{n}$ is the outward versor of $\partial Y_l$ surface;
- $\partial Y_l$ is defined in Figure 1**;**
- $[\![\boldsymbol{\sigma}]\!]$ is the jump of micro-stresses across any discontinuity surface of normal $\mathbf{n}^{\text{int}}$;
- $S^{\text{m}}$ and $S^{\text{b}}$ denote respectively the strength domains of mortar and bricks;
- $Y$ is the cross section of the 3D elementary cell with $y_3 = 0$ (see Figure 1), $|Y|$ is its area, $V$ is the elementary cell, $h$ represents the wall thickness and $y = (y_1 \quad y_2 \quad y_3)$.

In order to simply solve problem ( 1 ), the unit cell is subdivided into a fixed number of layers along its thickness, as shown in Figure 2-a. According to classical limit analysis plate models, for each layer out-of-plane components $\sigma_{i3}$ $(i = 1, 2, 3)$ of the micro-stress tensor $\boldsymbol{\sigma}$ are set to zero, so that only in-plane components $\sigma_{ij}$ $(i, j = 1, 2)$ are considered in the optimization.

Then, $\sigma_{ij}$ $(i, j = 1, 2)$ are kept constant along the $\Delta_{Li}$ thickness of each layer. As proposed by the authors for in-plane actions [11], for each layer one-fourth of the REV is sub-divided into nine geometrical elementary entities (*sub-domains*), so that all the cell is sub-divided into 36 sub-domains (Figure 2-b).

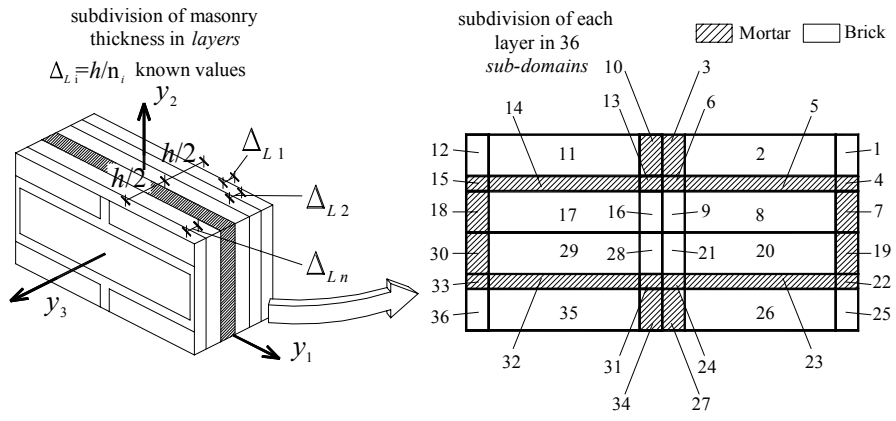


-a -b

Figure 2: The micro-mechanical model proposed. -a: subdivision in layers along the thickness. –b: subdivision of each layer in sub-domains

Inside each sub-domain $(k)$ and layer $(i_L)$, polynomial distributions of degree *(m)* are assumed for the stress components. Being stress fields polynomial expressions, the generic *ij*th component of the stress tensor can be written as follows:

$$\sigma_{ij}^{(k,i_L)} = \mathbf{X}(\mathbf{y})\mathbf{S}_{ij}^{(k,i_L)T} \qquad \mathbf{y} \in Y^{(k,i_L)} \tag{2}$$

where:

- $\mathbf{X}(\mathbf{y}) = \begin{bmatrix} 1 & y_1 & y_2 & y_1^2 & y_1 y_2 & y_2^2 & \dots \end{bmatrix}$;
- $\mathbf{S}_{ij}^{(k,i_L)} = \begin{bmatrix} S_{ij}^{(k,i_L)(1)} & S_{ij}^{(k,i_L)(2)} & S_{ij}^{(k,i_L)(3)} & S_{ij}^{(k,i_L)(4)} & S_{ij}^{(k,i_L)(5)} & S_{ij}^{(k,i_L)(6)} & \dots \end{bmatrix}$ is a vector representing the unknown stress parameters of sub-domain $(k)$ of layer $(i_L)$;
- $Y^{(k,i_L)}$ represents the $k^{\text{th}}$ sub-domain of layer $(i_L)$.

The imposition of equilibrium inside each sub-domain, the continuity of the stress vector on interfaces and the anti-periodicity of $\boldsymbol{\sigma}\mathbf{n}$ permit a strong reduction of the total number of independent stress parameters.

For instance, the imposition of micro-stress equilibrium ($\sigma_{ij,j} = 0 \quad i = 1,2$) in each sub-domain yields:

$$\sum_{j=1}^{2} \mathbf{X}(\mathbf{y})_{,j} \mathbf{S}_{ij}^{(k,i_L)T} = \mathbf{0} \tag{3}$$

If $p$ is the degree of the polynomial expansion, $p(p+1)$ equations can be written.

A further reduction of the total unknowns is obtained imposing the continuity of the (micro)-stress vector on internal interfaces ($\sigma_{ij}^{(k,i_L)} n_j^{\text{int}} + \sigma_{ij}^{(r,i_L)} n_j^{\text{int}} = 0 \quad i = 1,2$) for every $(k,i_L)$ and $(r,i_L)$ contiguous sub-domains with a common interface of normal $\mathbf{n}^{\text{int}}$. Other $2(p+1)$ equations in the stress coefficients can be written for each interface as follows:

$$\left( \hat{\mathbf{X}}_{ij}^{(k,i_L)}(\mathbf{y}) \hat{\mathbf{S}}^{(k,i_L)} + \hat{\mathbf{X}}_{ij}^{(r,i_L)}(\mathbf{y}) \hat{\mathbf{S}}^{(r,i_L)T} \right) n_j^{\text{int}} = 0 \quad i = 1,2 \tag{4}$$

Furthermore, anti-periodicity of $\boldsymbol{\sigma}\mathbf{n}$ on $\partial V$ requires other $2(p+1)$ equations per pair of external faces $(m,i_L)$ and $(n,i_L)$, i.e. it should be imposed that stress vectors $\boldsymbol{\sigma}\mathbf{n}$ are opposite on opposite sides of $\partial V$:

$$\hat{\mathbf{X}}_{ij}^{(m,i_L)}(\mathbf{y}) \hat{\mathbf{S}}^{(m,i_L)} \mathbf{n}_{1,j} = -\hat{\mathbf{X}}_{ij}^{(n,i_L)}(\mathbf{y}) \hat{\mathbf{S}}^{(n,i_L)} \mathbf{n}_{2,j} \tag{5}$$

Where $\mathbf{n}_1$ and $\mathbf{n}_2$ are oriented versors of the external faces of the paired sub-domains $(m,i_L)$ and $(n,i_L)$.

After some trivial elementary assemblage operations on the local variables, stress vector of layer $i_L$ inside sub-domain $(k)$ can be written as follows:

$$\tilde{\boldsymbol{\sigma}}^{(k,i_L)} = \tilde{\mathbf{X}}^{(k,i_L)}(\mathbf{y}) \tilde{\mathbf{S}}^{(i_L)} \tag{6}$$

Where $\widetilde{\mathbf{S}}^{(i_L)}$ is the vector of unknown stress parameters of layer $i_L$.

As it has been show for the in-plane case by the authors [11], reliable results can be obtained if a fourth order polynomial expansion is chosen for the stress field. For this reason, in what follows, expansions of degree four are adopted.

Once fixed the polynomial degree, the out-of-plane model presented requires a subdivision ($n_L$) of the wall thickness into several layers (Figure 2-a), with an a-priori fixed constant thickness $\Delta_{L_i} = t / n_L$ for each layer. In this way, the following simple (non) linear optimization problem is derived:

$$
\begin{cases}
\max\{\lambda\} & \\
\begin{cases}
\mathbf{N} = \int_{k,i_L} \widetilde{\boldsymbol{\sigma}}^{(k,i_L)} dV & (a) \\
\mathbf{M} = \int_{k,i_L} y_3 \widetilde{\boldsymbol{\sigma}}^{(k,i_L)} dV & (b) \\
\mathbf{M} = \begin{bmatrix} M_{xx} & M_{xy} \\ M_{xy} & M_{yy} \end{bmatrix} = \lambda \begin{bmatrix} \cos(\psi)\cos(\vartheta) & \sin(\vartheta) \\ \sin(\vartheta) & \sin(\psi)\cos(\vartheta) \end{bmatrix} & (c) \\
\psi = [0; 2\pi] \quad \theta = [0; \pi/2] & (d) \\
\widetilde{\boldsymbol{\sigma}}^{(k,i_L)} = \widetilde{\mathbf{X}}^{(k,i_L)}(\mathbf{y})\widetilde{\mathbf{S}} & (e) \\
\widetilde{\boldsymbol{\sigma}}^{(k,i_L)} \in S^{(k,i_L)} & (f) \\
k = 1, \ldots, \text{ number of } sub-domains; \; i_L = 1, \ldots, \text{number of } layers & (g)
\end{cases} & \text{such that}
\end{cases}
\qquad (7)
$$

where:

- $\lambda$ is the ultimate bending moment with directions $\psi$ and $\vartheta$ in the $M_{xx} - M_{yy} - M_{xy}$ space;
- $\psi$ and $\vartheta$ are spherical angles in $M_{xx} - M_{yy} - M_{xy}$, given by $\tan(\vartheta) = \dfrac{M_{xy}}{\sqrt{(M_{xx}^2 + M_{yy}^2)}}$, $\tan(\psi) = \dfrac{M_{yy}}{M_{xx}}$;
- $S^{(k,i_L)}$ denotes the (non-linear) strength domain of the constituent material (mortar or brick) corresponding to the $k^{th}$ sub-domain and $i_L^{th}$ layer;
- $\widetilde{\mathbf{S}}$ collects all the unknown polynomial coefficients (of each sub-domain of each layer).

For the sake of simplicity, membrane actions are kept constant and independent from load multiplier. In this way, in-plane actions affect optimization only in the evaluation of $M_{xx}, M_{yy}, M_{xy}$ strength domains. This assumption is technically acceptable for the experimental tests analyzed next, since in these cases a fixed in-plane compressive load (if present) $N_{yy} = -N_0$ is applied before out-of-plane actions and kept constant until failure, whereas $N_{xx} = N_{xy} = 0$.

Finally, we refer the reader to classical papers [12] [13] for a critical discussion both on the procedures adopted to reduce ( 7 ) to a linear programming problem and on the algorithms used (based on the revised simplex method) to solve efficiently the linearized problem derived from ( 7 ).

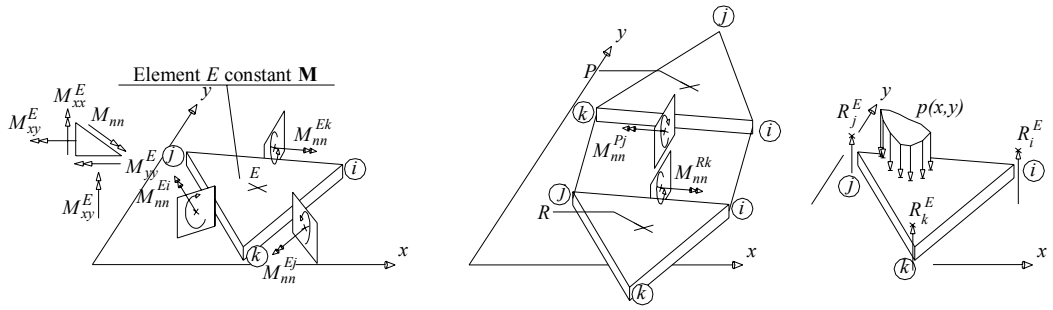


Figure 3: Triangular plate element used for the lower bound FE limit analysis (-a), continuity of the bending moment on interfaces (-b), integral equilibrium (-c)

# 3 Lower and upper bound FE limit analysis of slabs

In this section, the finite elements utilized next for the lower and upper bound limit analyses are briefly recalled.

## 3.1 Lower bound approach

A FE lower bound limit analysis program based on the triangular plate bending element proposed independently by Hellan and Herrmann [5] [6] has been implemented using Matlab™. This triangular element has been chosen for its simplicity and for the very reduced number of unknowns involved in the optimization.

A constant moment field is assumed inside each element $E$, so that three moment unknowns per element are introduced; such unknowns are the horizontal, vertical and torsion moments ($M^E_{xx}, M^E_{yy}, M^E_{xy}$) or alternatively three bending moments $M^{Ei}_{nn}$, $M^{Ej}_{nn}$, $M^{Ek}_{nn}$ along the edges of the triangle (Figure 3-a).

Continuity of $M^E_{nn}$ bending moments is imposed for each internal interface between two adjacent elements $R$ and $P$ (i.e. $M^{Rk}_{nn} = M^{Pj}_{nn}$, see Figure 3-b), whereas no constraints are imposed for the torsion moment and the shear force.

Internal equilibrium for each element is ensured only in integral form, due to the constant assumption for the moments field. By means of the principle of virtual work, three equilibrium equation for each triangle are obtained (see [14] for details):

$$\mathbf{R}_E + \mathbf{B}_E^T \mathbf{M}_E = \mathbf{P}_E \qquad (8)$$

where:

- $\mathbf{R}_E = \begin{bmatrix} R_i & R_j & R_k \end{bmatrix}^T$ are nodal (unknown) reactions see Figure 3-c;

- $\mathbf{B}_E = \frac{1}{2A_E}\begin{bmatrix} \frac{b_i b_i + c_i c_i}{l_i} & \frac{b_i b_j + c_i c_j}{l_i} & \frac{b_i b_k + c_i c_k}{l_i} \\ \frac{b_j b_i + c_j c_i}{l_j} & \frac{b_j b_j + c_j c_j}{l_j} & \frac{b_j b_k + c_j c_k}{l_j} \\ \frac{b_k b_i + c_k c_i}{l_k} & \frac{b_k b_j + c_k c_j}{l_k} & \frac{b_k b_k + c_k c_k}{l_k} \end{bmatrix}$, with $b_i = y_j - y_k$,
  $c_i = x_k - x_j$ ad $A_E$ element area;
- $\mathbf{P}_E = \frac{1}{2A_E}\mathbf{T}_E^T \int_E [1 \quad x \quad y]^T p(x,y) dA$ ($\mathbf{T}_E^T = \begin{bmatrix} a_i & a_j & a_k \\ b_i & b_j & b_k \\ c_i & c_j & c_k \end{bmatrix}, a_i = x_j y_k - x_k y_j$).

In order to ensure nodal equilibrium, further equilibrium conditions should be imposed. For each (not-constrained) node $i$ $\sum_{r=1}^{p} R_i^E = 0$, where $R_i^E$ is referred to element $E$ and $p$ is the number of elements with one vertex in $i$.

For each element $E$ only one admissibility condition in the linearized form $\mathbf{A}_E^{in}\mathbf{M}_E \le \mathbf{b}_{in}^E$ is required, where $\mathbf{A}_E^{in}$ is a $mx3$ coefficients matrix of the linearization planes of the strength domain, $m$ is the number of the planes in the linearization, $\mathbf{b}_{in}^E$ collects the right hand sides of these planes and $\mathbf{M}_E = \left[M_{xx}^E \quad M_{yy}^E \quad M_{xy}^E\right]^T$ is the vector of element unknown moments.

After some elementary assemblage operations, the following linear programming problem is obtained:

$$\max\left\{\lambda \mid \mathbf{A}^{eq}\mathbf{M} = \mathbf{b}^{eq};\ \mathbf{A}^{in}\mathbf{M} \le \mathbf{b}^{in}\right\} \qquad (9)$$

Where $\lambda$ is the limit multiplier, $\mathbf{M}$ is the (assembled) vector of moment unknowns (three for each element), $\mathbf{A}^{eq}\mathbf{M} = \mathbf{b}^{eq}$ collects elements equilibrium, continuity of the bending moment on interfaces and nodal equilibrium, whereas $\mathbf{A}^{in}\mathbf{M} \le \mathbf{b}^{in}$ collects linearized yield conditions ($mxN^{el}$ inequalities if $N^{el}$ is the number of elements).

## 3.2 Upper bound approach

A FE upper bound limit analysis program based on the triangular element proposed by Munro and Da Fonseca [7] has been implemented using Matlab™. The displacement field is kept linear inside each element and nodal velocities are taken as optimization variables.

If $\mathbf{w}_E = \left[w_i^E \quad w_j^E \quad w_k^E\right]^T$ are element $E$ nodal velocities and $\boldsymbol{\theta}_E = \left[\vartheta_i^E \quad \vartheta_j^E \quad \vartheta_k^E\right]^T$ are side normal rotations, $\boldsymbol{\theta}_E$ and $\mathbf{w}_E$ are linked by the

compatibility equation $\boldsymbol{\theta}_E = \mathbf{B}_E \mathbf{w}_E$. Plastic dissipation occurs only along each interface $I$ between two adjacent triangles $R$ and $K$ or on a boundary side $B$ of an element $Q$ (see Figure 4).

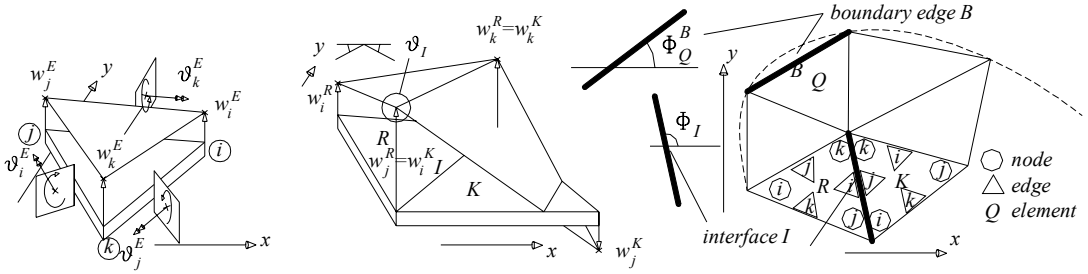


-a -b -c

Figure 4: Triangular plate element used for the upper bound FE limit analysis (-a), rotation along an interface between adjacent triangles (-b), discretization of the 2D domain (-c)

Internal power $P_I^{in}$ dissipated along $I$ can be written as follows:

$$\begin{aligned} P_I^{in} &= M_{nn,I}^{+} \vartheta_I \quad \vartheta_I > 0 \\ P_I^{in} &= M_{nn,I}^{-} \left|\vartheta_I\right| \quad \vartheta_I < 0 \end{aligned} \qquad (10)$$

where:

- $\vartheta_I = \vartheta_i^R + \vartheta_j^K$ is the relative rotation between $R$ and $K$ along $I$ (see Figure 4);
- $M_{nn,I}^{+}$ and $M_{nn,I}^{-}$ are positive and negative failure bending moments along $I$; a rigorous upper bound of the collapse load can be obtained deducing $M_{nn,I}^{+}$ and $M_{nn,I}^{-}$ from the actual strength domain ($S^{\hom}$) of the homogenized material in the space $M_{xx} - M_{yy} - M_{xy}$ by means of the following optimization:
  $M_{nn,I}^{+} = -M_{nn,I}^{-} = \max\left\{ M_{nn} \mid M_{nn} = M_{xx}\sin^2\Phi_I + M_{yy}\cos^2\Phi_I - M_{xy}\sin(2\Phi_I) \right\}$, where $\left[M_{xx} \quad M_{yy} \quad M_{xy}\right] \in S^{\hom}$
  $\Phi_I$ is the interface rotation angle with respect to the horizontal direction. A similar expression can be obtained for a boundary side $B$ of an element $Q$, with the only difference that in this case $\Phi_I = \Phi_i^Q$.

Since the internal power dissipated $P^{in} = \sum_{i^I}^{n^I} P_{i^I}^{in} + \sum_{i^B}^{n^B} P_{i^B}^{in}$, from equation (10) a non linear optimization problem is derived. This non linearity can be easily avoided introducing positive and negative rotations as follows: $P_I^{in} = M_{nn,I}^{+}\vartheta_I^{+} + M_{nn,I}^{-}\vartheta_I^{-} \quad \vartheta_I = \vartheta_I^{+} - \vartheta_I^{-} \quad \vartheta_I^{+}; \vartheta_I^{-} \geq 0$.

External power dissipated can be written as $P^{ex} = \left(\mathbf{P}_0^T + \lambda \mathbf{P}_1^T\right)\mathbf{w}$, where $\mathbf{P}_0$ is the vector of (lumped) permanent loads, $\lambda$ is the load multiplier, $\mathbf{P}_1^T$ is the vector of (lumped) variable loads and $\mathbf{w}$ is the vector of assembled nodal velocities. As the amplitude of the failure mechanism is arbitrary, a further normalization condition $\mathbf{P}_1^T \mathbf{w} = 1$ is usually introduced. Hence, the external power becomes linear in $\mathbf{w}$ and $\lambda$, i.e. $P^{ex} = \mathbf{P}_0^T \mathbf{w} + \lambda$.

After some elementary assemblage operations, the following optimization problem is derived:

$$\min\left\{\mathbf{M}^{+T}\boldsymbol{\theta}^{+} + \mathbf{M}^{-T}\boldsymbol{\theta}^{-} - \mathbf{P}_0^T\mathbf{w} \mid \boldsymbol{\theta}^{+} - \boldsymbol{\theta}^{-} = \mathbf{B}\mathbf{w};\ \boldsymbol{\theta}^{+} \geq \mathbf{0};\ \boldsymbol{\theta}^{-} \geq \mathbf{0};\ \mathbf{P}_1^T\mathbf{w} = 1\right\} \qquad (11)$$

where;

- $\mathbf{M}^{+}$ and $\mathbf{M}^{-}$ vectors collect positive and negative failure bending moments along interfaces and boundary sides;
- $\boldsymbol{\theta}^{+}$ and $\boldsymbol{\theta}^{-}$ vectors collect positive and negative interface and boundary rotation angles;
- $\mathbf{B}$ is a geometrical matrix built up assembling $\mathbf{B}_E$ element matrices, already introduced in the previous section.

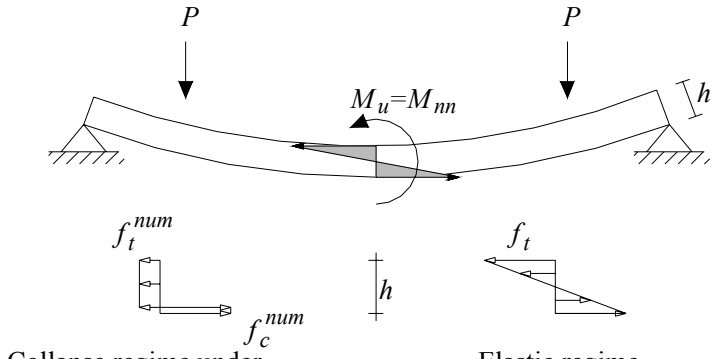


Figure 5: Uniaxial tensile strength from known values of failure moment $M_u$ in four point bending. –a: collapse stress distribution, perfect plasticity (present model). –b: experimental procedure (elastic properties of section)

# 4 Structural examples

In this section, the homogenized model previously presented is validated by means of some comparisons with experimental data on entire masonry panels out-of-plane loaded.

It is stressed that experimental data available from different authors are reported in terms of maximum bending moments or flexural tensile strengths along horizontal and vertical directions. Usually, flexural tensile strengths $f_t$ are quantities derived from experimental failure moments $M_u$ by means of the elastic relation $f_t = M_u / W_{el} = 6M_u /(bh^2)$, see also Figure 5-b, where $h$ is the wall thickness and $b$ is a unitary length. Of course, these values of $f_t$ are not the real uniaxial tensile strengths. A more realistic stress distribution along the thickness of the wall at failure (under the assumption of perfect plasticity for the constituent materials) is depicted in Figure 5-a. This implies that mechanical properties to adopt for mortar and units in the homogenization model have to be chosen in order to fit horizontal and vertical uniaxial tensile strengths of Figure 5-a, i.e. experimental values divided roughly by 3 (see also stress/strain diagrams of EC6 code [4]).

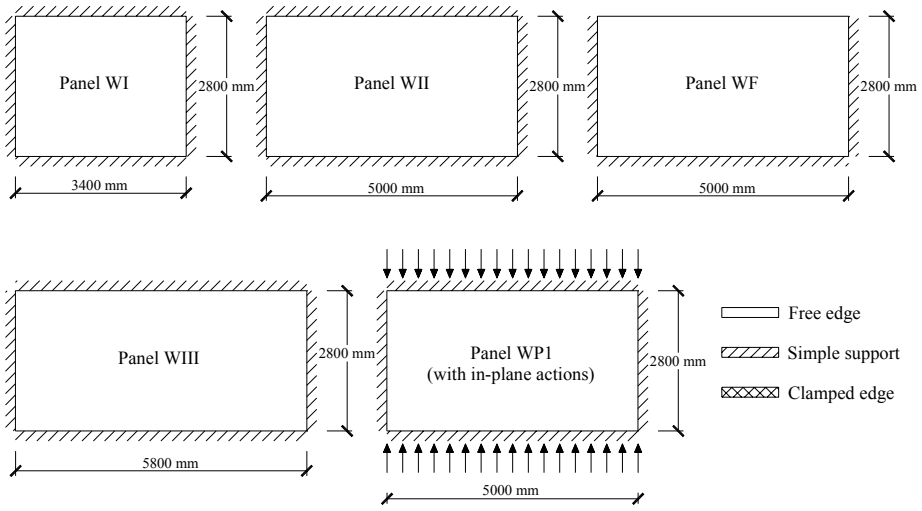


Figure 6: Gazzola et al. [9] experimental tests on out of-plane loaded masonry walls. Panel dimensions and boundary conditions

The panels here analyzed consist of hollow concrete block masonry. The tests were carried out by Gazzola et al. [9] and are denoted by W. Five panels were tested by the authors (WI, WII, WF, WIII, WP1), as shown in Figure 6. The panels were loaded until failure with increasing out-of-plane uniform pressure $p$. For each configuration, three different tests were carried out and the results reported by the authors represent the average of the tests. The only panel with in-plane action was WP1, which was loaded, previously to the application of the out-of-plane loading, with an in-plane confining vertical pressure of $0.2\ N/mm^2$.

In this paper, for the sake of conciseness, only panels WII and WF are analyzed with the homogenized model at hand. With reference to the incremental non-linear analysis conducted by Lourenço in [15] and [16], these panels have a relatively ductile behavior and therefore are suitable for a homogenized limit analysis.

| *Mortar* | *Brick* |
|---|---|
| Mohr Coulomb plane strain with tension cut-off | Compression cut-off |
| $f_{tm} = 0.157 \frac{N}{mm^2}$ (tension cut-off)<br>$c_m = 3.8 f_{tm}$ (cohesion), $\Phi_m = 36°$ (friction angle) | $f_{cb} = 22.7 \frac{N}{mm^2}$ |

Table 1: Mechanical characteristics adopted in the homogenisation model for joints and bricks, out-of-plane loaded panels by Gazzola et al. [9]

Inelastic properties of mortar and bricks are reported in Table 1 and are chosen in order to fit experimental vertical/horizontal masonry strengths reported by Gazzola et al. [9] divided by three. The homogenized failure surface obtained solving problem ( 7 ) for several directions of $\lambda$ is reported in Figure 7**.**

Figure 8 shows a comparison among the failure loads obtained numerically (both upper and lower bound methods), the load-displacement diagrams obtained by Lourenço in [15] and [16] and experimental failure loads. It is worth noting that no information is available from Gazzola et al. [9] regarding experimental load-displacement diagrams, as well as about the scatter of the tests.

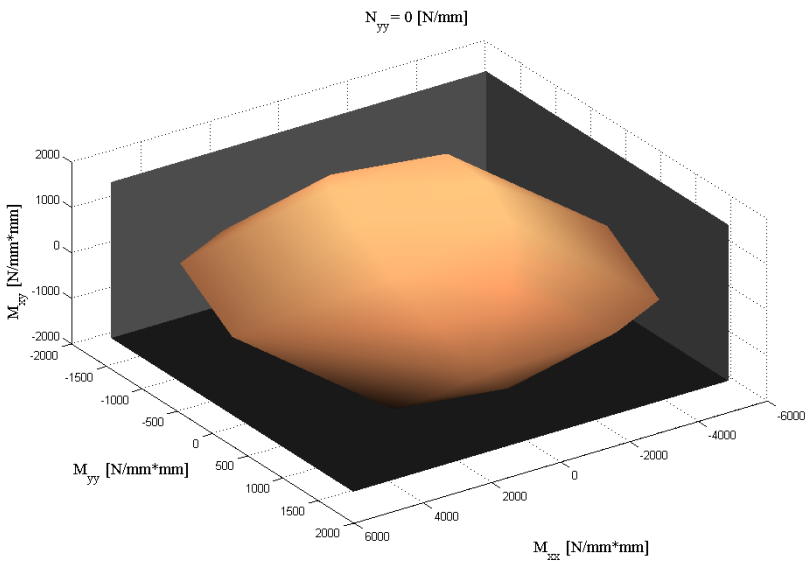


Figure 7: Homogenized failure surface for Gazzola et al. [9] tests

Finally, in Figure 9 principal moments distribution at collapse from the lower bound analysis for panel WF and failure mechanism (with the relative mesh used) from the upper bound analysis are reported. The comparison shows that reliable predictions can be obtained using the homogenized model proposed.

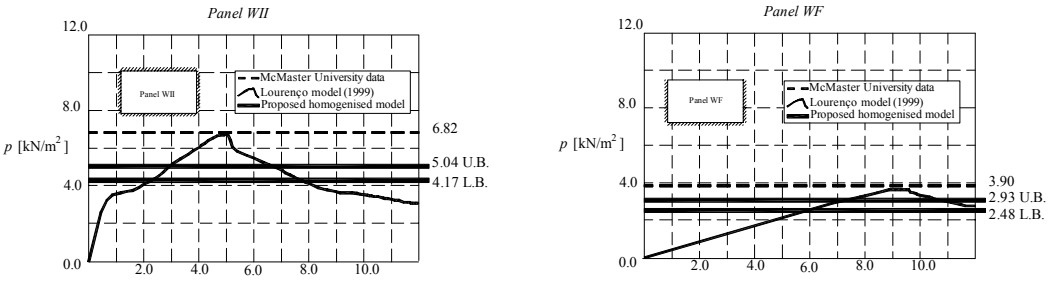


Figure 8: Comparison between experimental and numerical results, Gazzola et al. [9] tests, panels WII and WF

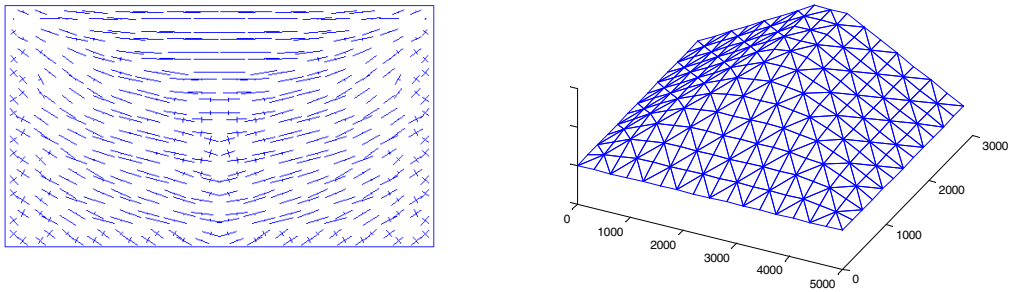


-a -b

Figure 9: Gazzola et al. [9] experimental tests, lower and upper bound FE limit analysis results. –a: Principal moments at collapse, panel WF, -b: failure mechanism from the upper bound FE limit analysis and mesh used, panel WF

# 5 Conclusions

In the present paper, a novel micro-mechanical model for the homogenized limit analysis of masonry walls subjected to out-of-plane actions has been presented. Adopting a polynomial expansion for the stress fields and subdividing into several layers masonry thickness, a simple linear optimisation problem has been derived on the elementary cell with the aim to find brickwork homogenised failure surfaces.

The homogenised failure surfaces so recovered have been implemented in FE limit analysis codes and meaningful structural examples have been treated in detail both with a lower and an upper bound approach.

The comparisons both with experimental data and previously developed incremental numerical procedures have shown that reliable results can be obtained by means of the micro-mechanical model proposed.

# References


[1] R. Spence, A. Coburn, “Strengthening building of stone masonry to resist earthquakes”, Meccanica, 27, 213-221, 1992.

[2] B.P. Sinha, “A simplified ultimate load analysis of laterally loaded model orthotropic brickwork panels of low tensile strength”, J. Struct. Eng. ASCE, 56B(4), 81-84, 1978.

[3] British Standard Institution, “BS 5628 part I: Use of Masonry 1978; BS 5628 part II: Use of Masonry 1985; BS 5628 part III: Use of Masonry 1985”.

[4] EN 1996. Euro Code 6: Design of masonry structures.

[5] K. Hellan, “Analysis of elastic plates in flexure by a simplified finite element method”, Acta Polytech. Scand., Trondheim, Ci 46, 1-28, 1967.

[6] L.R. Herrmann, “Finite element bending analysis for plates”, J. Eng. Mech. Div. ASCE, 93, 13-26, 1967.

[7] J. Munro, A.M.A. Da Fonseca, “Yield-line method by finite elements and linear programming”, J. Struct. Eng. ASCE, 56B, 37-44, 1978.

[8] E.A. Gazzola, R.G. Drysdale, “A component failure criterion for blockwork in flexure”, Structures ‘86 ASCE, edited by S.C. Anand, New Orleans, Louisiana, USA, 134-153, 1986.

[9] E.A. Gazzola, R.G. Drysdale, A.S. Essawy, “Bending of concrete masonry walls at different angles to the bed joints”, Proc. 3th North. Amer. Mas. Conf., Arlington, Texas, USA, Paper 27, 1985.

[10] P. Suquet, “Analyse limite et homogeneisation”, Comptes Rendus de l'Academie des Sciences - Series IIB – Mechanics, 296, 1355-1358, 1983.

[11] G. Milani, P.B. Lourenço, A. Tralli, “Homogenized limit analysis of masonry walls. Part I: failure surfaces”, Submitted Computers & Structures, 2005.

[12] E. Anderheggen, H. Knopfel, “Finite element limit analysis using linear programming”, International Journal of Solids and Structures, 8, 1413-1431, 1971.

[13] G. Maier, “Mathematical programming methods for deformation analysis at plastic collapse”, Computers and Structures, 7, 599-612, 1977.

[14] A.A. Cannarozzi, M. Capurso, F. Laudiero, “An iterative procedure for collapse analysis of reinforced concrete plates”, Computer Methods in Applied Mechanics and Engineering, 16, 47-68, 1978.

[15] P.B. Lourenço, “An anisotropic macro-model for masonry plates and shells: implementation and validation”, Report 03.21.1.3.07, University of Delft, Delft, Holland and University of Minho, Guimarães, Portugal, 1997.

[16] P.B. Lourenço, “Anisotropic softening model for masonry plates and shells”, Jour. Struct. Eng. ASCE, 126(9), 1008-1016, 1999.